Review Article | Intervention

http://dx.doi.org/10.3348/kjr.2015.16.1.114
pISSN 1229-6929 · eISSN 2005-8330
Korean J Radiol 2015;16(1):114-124

Korean Journal of Radiology
KJR

Role of C-Arm Cone-Beam CT in Chemoembolization for Hepatocellular Carcinoma

Hyo-Cheol Kim, MD

Department of Radiology, Seoul National University College of Medicine, Institute of Radiation Medicine, Seoul National University Medical Research Center, and Clinical Research Institute, Seoul National University Hospital, Seoul 110-744, Korea

With the advent of C-arm cone-beam computed tomography (CBCT), minimally-invasive procedures in the angiography suite made a new leap beyond the limitations of 2-dimensional (D) angiography alone. C-arm CBCT can help interventional radiologists in several ways with the treatment of hepatocellular carcinoma (HCC); visualization of small tumors and tumor-feeding arteries, identification of occult lesion and 3D configuration of tortuous hepatic arteries, assurance of completeness of chemoembolization, suggestion of presence of extrahepatic collateral arteries supplying HCCs, and prevention of nontarget embolization. With more improvements in the technology, C-arm CBCT may be essential in all kinds of interventional procedures in the near future.

Index terms: *Hepatocellular carcinoma; Chemoembolization; C-arm cone-beam CT*

INTRODUCTION

Chemoembolization is a widely used palliative treatment modality for inoperable hepatocellular carcinoma (HCC) (1). To perform chemoembolization safely and effectively, it is essential to achieve selective catheterization of the tumor-feeding branch based on a thorough knowledge of the hepatic artery and extrahepatic collateral arteries. However, multiple angiographic runs are needed to identify small tumor-feeding branches because multiple hepatic arteries overlap each other. In addition, there are several hypervascular non-tumorous stainings mimicking HCCs and fine non-hepatic arteries arising from the hepatic artery, which may cause complications if inadvertent or intentional embolization is undertaken.

C-arm cone-beam computed tomography (CBCT) technology using a flat-panel detector (FPD) is a useful tool for obtaining cross-sectional and three-dimensional (3D) images during interventional procedures. This technique has been popularly used in various interventional procedures such as adrenal vein sampling, transjugular intrahepatic portosystemic shunts, transthoracic needle biopsy, and chemoembolization for HCC (2-4). In intra-arterial treatment for HCC, C-arm CBCT can provide additional crucial information, including visualization of small tumors and their feeding-arteries, non-hepatic arteries, and possibly of extrahepatic collateral arteries. Recent potent intra-arterial treatment modalities such as drug-eluting beads and Y-90 radioactive beads may cause serious complications when non-hepatic arteries are treated (5). Thus, C-arm CBCT has become an inevitable tool for safe and favorable clinical outcomes. The purpose of this article is to review the technology of C-arm CBCT and its role in chemoembolization for HCC.

Received May 26, 2014; accepted after revision October 9, 2014.
Corresponding author: Hyo-Cheol Kim, MD, Department of Radiology, Seoul National University Hospital, 101 Daehak-ro, Jongno-gu, Seoul 110-744, Korea.
• Tel: (822) 2072-2584 • Fax: (822) 743-7418
• E-mail: angiointervention@gmail.com

Korean Journal of Radiology
KJR

Terminology

Digital technology launched FPD instead of the image intensifier system. The FPD provides markedly improved contrast and spatial resolution compared to image intensifier system. Whereas conventional multidetector CT (MDCT) adopts a fan-beam geometry and is equipped with multiple one-dimensional detectors, CBCT obtains information using cone-beam geometry and a two-dimensional (2D) FPD, which make it possible to generate a whole volumetric data set in a single gantry rotation. Thus, recent angiographic machines have CBCT mounted on a C-arm.

Various terms have described these new volumetric imaging systems in the literature, including C-arm CT, cone-beam CT, angiographic CT, volume CT, and flat-panel CT. In this article, the term C-arm CBCT will be used to refer to C-arm-mounted CBCT using a digital FPD.

Resolution

In MDCT, detector row width ranges from 0.5 mm to 0.6 mm for the current 64-slice scanners and the patient is scanned in a helical fashion. An isotropic voxel size of 0.5 x 0.5 x 0.5 mm^3 can be obtained with current state-of-the-art MDCT. For C-arm CBCT systems, current detector arrays are 40 x 30 cm^2, allowing 25 x 25 x 18 cm^3 volumetric datasets to be generated. Isotropic voxel sizes of under 0.2 x 0.2 x 0.2 mm^3 can be theoretically achievable with current C-arm CBCT systems. This higher spatial resolution of C-arm CBCT can make it possible to observe very thin subsegmental hepatic arteries which may not be discernible on CT hepatic arteriography using MDCT (Fig. 1).

The contrast resolution of C-arm CT in delineating soft-tissue structures is notably lower than that of MDCT owing to the increased beam scatter generated by the C-arm angiographic system compared with the conventional MDCT scanner (6). Whereas MDCT has approximately 3 Hounsfield units (HU) contrast resolution, CBCT allows a contrast resolution of 10 HU.

Protocol

Three C-arm CBCT systems are commercially available in Korea: DynaCT (Siemens Medical Solutions, Forchheim, Germany), XperCT (Philips Medical Systems, Eindhoven, the Netherlands), and Innova CT (GE Healthcare, Waukesha, WI, USA). Each of these systems has its own imaging protocol, in addition to different rotation times, numbers of projections acquired, image quality, image reconstruction time, and dedicated post-processing programs. In our hospital, DynaCT is available for chemoembolization, and the parameters of the C-arm CBCT scan are 0.5° increment, 512 x 512 matrix in projections, total angle of 211° at approximately 26° per second, a total of 419 projections, and an 8-second scan time. Recent C-arm CBCT machines

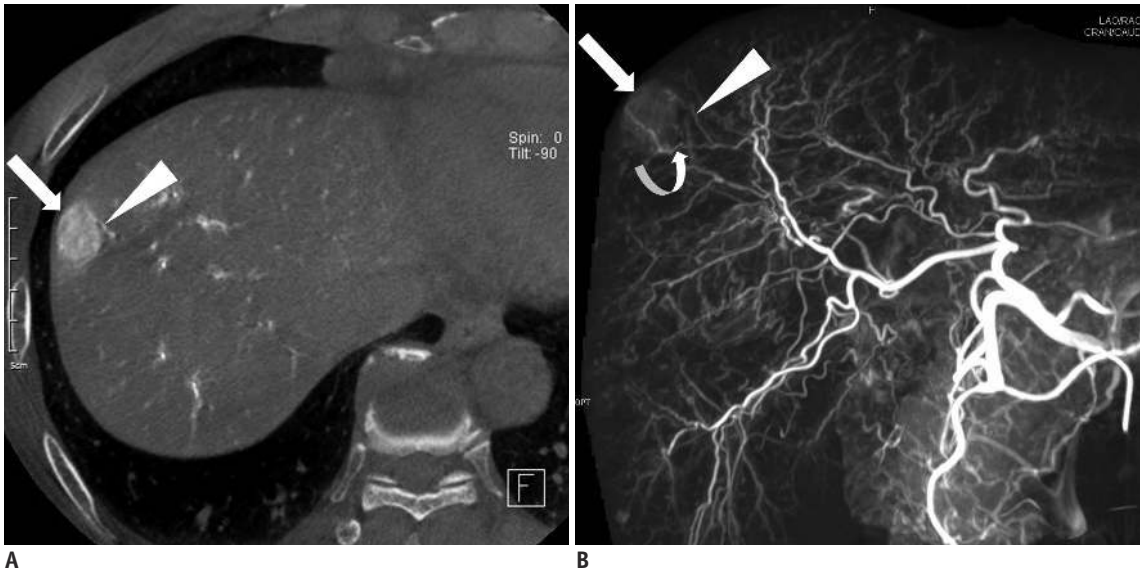

A B

Fig. 1. 60-year-old man with hepatocellular carcinoma.
A. C-arm cone-beam CT shows nodular tumor (arrow) supplied by adjacent subsegmental hepatic artery (arrowhead). **B.** Maximum intensity projection image of C-arm cone-beam CT obtained at common hepatic artery shows small nodular tumor (arrow) supplied by subsegmental hepatic artery (arrowhead) which was noted on axial image **(A)**. Note another subsegmental hepatic artery (curved arrow) feeding nodular tumor.

only require a 5-second scan time.

The following are typical imaging process using C-arm CBCT for chemoembolization in our institution. C-arm CBCT is obtained at the proper hepatic artery or common hepatic artery by using a 5-Fr catheter (RH, Cook, Bloomington, IN, USA) or 2.6-Fr microcatheter (Asahi Intecc, Aichi, Japan). When the tip of the 5-Fr catheter can be advanced into the common hepatic artery, the C-arm CBCT is obtained by using 5-Fr catheter. When the tip of 5-Fr catheter cannot be advanced into the common hepatic artery, the C-arm CBCT is obtained by using 2.6-Fr microcatheter placed in the proper hepatic artery. In patients with hepatic artery variation (i.e., replaced right hepatic artery from the superior mesenteric artery or replaced left hepatic artery from the left gastric artery), an additional C-arm CBCT is obtained by using 2.0–2.6-Fr microcatheter placed in the replaced right or left hepatic artery. The injection rate of the contrast media is 3–4 mL/sec at the proper or common hepatic artery and 1.5–2.5 mL/sec at the right or left hepatic artery according to the vessel size and catheter size used. The preferred scan delay is 4 seconds, which means that scanning is initiated 4 seconds after the start of contrast material injection. Iodinated contrast media (Pamiray 300; Dongkook, Seoul, Korea) is used without dilution. C-arm CBCT images are reviewed on a dedicated workstation by multiplanar reformation images, maximum-intensity projection images, and volume-rendering images.

Most of the parameters of the C-arm CBCT are fixed according to the machines used, but two parameters can be adjusted by operators; scan delay and contrast media dilution. In most literature, scan delay ranges from 3 seconds to 8 seconds. A 4 second scan delay was recommended by Tognolini for better hepatic arterial visualization (7), and a 6 second scan delay was used for better visualization of small tumors (8). To optimize the image quality of C-arm CBCT, scan delay should be tailored to individual patients, considering the blood flow velocity through the hepatic artery and the position of the tip of catheter. A 6 second or more scan delay may be contaminated by portal vein enhancement, while a 3 second or less scan delay may not be enough to obtain sufficient enhancement of tumors.

Most interventional radiologists prefer half dilution of contrast media in C-arm CBCT imaging. Half-diluted contrast media (150–175 mg/mL as iodide) may reduce beam-hardening artifacts. However, according to our clinical experience, thin subsegmental hepatic arteries may be obscure when diluted contrast media is used, so undiluted contrast media (300 mg/mL as iodide) is preferred in our institute. The optimal concentration of iodine in contrast media for chemoembolization should be further studied. If contrast media diluted to 100 mg iodine/mL is used, longer scan delay (8 seconds) is needed to acquire adequate tumor-to-liver contrast (9).

The recent dual-phase CBCT prototype, which is vendor specific, allows two sequential scans, which can obtain CBCT images of both arterial and venous phases by using only one contrast material injection. The venous phase of the C-arm CBCT is useful to identify corona enhancement (10). Corona enhancement indicates venous drainage through hypervascular HCC nodules and can discriminate HCC from arterioportal shunts. Dual phase C-arm CBCT depicted corona enhancement in 88.7% of small tumors and diagnostic accuracy of small HCC nodules can be improved (10). With dual phase C-arm CBCT, tumor enhancement changes after chemoembolization using drug-eluting beads can be evaluated and is has been reported to serve as a useful prognostic indicator of short-term HCC response (11).

Benefit of C-Arm CBCT in Chemoembolization

Tumor Detection

There are many reports regarding detection rates of HCCs and their feeding arteries on C-arm CBCT with variable results. Detection rates of HCCs may depend on the tumor size, C-arm CBCT protocol, and gold standard. Generally, C-arm CBCT shows additional HCCs that are not evident on CT, MRI, and angiography, so the sensitivity of HCC detection is increased through the use of CBCT. But, non-tumorous lesions mimicking HCCs are frequently seen on C-arm CBCT, resulting in reduced specificity.

Although Higashihara et al. (12) reported that there was no significant difference between MDCT and C-arm CBCT in detection of HCCs, other researchers reported that C-arm CBCT has a higher sensitivity in detection of small HCCs compared to MDCT (13, 14). Meyer et al. (13) reported that CBCT showed high sensitivity and a high false-positive rate compared to MDCT. Iwazawa et al. (14) also reported that diagnostic accuracy was significantly higher using C-arm CBCT (Az = 0.830) as compared with MDCT (Az = 0.618) in the detection of HCCs smaller than 1 cm in diameter ($p < 0.001$), although the accuracy of the two techniques did not differ significantly for HCC lesions 1 cm or larger in diameter. C-arm CBCT was significantly more sensitive

Korean Journal of Radiology
KJR

than MDCT in the detection of lesions 20 mm or smaller (74.1% vs. 34.0% for lesions < 10 mm [$p < 0.001$]; 94.7% vs. 77.1% for lesions 10–20 mm [$p < 0.001$]) (14). In these studies (12-14), however, the standard of reference for the existence of HCC was only based on the results of blind readings of the MDCT images obtained before chemoembolization or the result of iodized accumulation one week later on CT, and the true positive proof of existence of HCC was unclear.

In daily clinical practice, small nodules less than 1.5 cm that are seen on CT or MRI may not be frequently observed on ultrasound and angiography, resulting in difficultly treating with radiofrequency ablation or chemoembolization, respectively. Miyayama et al. (15) reported that more than 95% of small tumors (mean size 1.3 cm) that were not detected by angiography could be seen on C-arm CBCT and 82% of those could be adequately treated by ultraselective chemoembolization.

Loffroy et al. (16) reported the detectability of HCCs at dual-phase CBCT was 93.9% compared with contrast-enhanced MRI. Since the reference standard of HCC detection was contrast-enhanced MRI using the gadolinium-based MRI contrast agent gadodiamide (Omniscan, GE Healthcare), they did not evaluate the possibility that HCCs that were not detected on MRI.

A recently published report has indicated that the diagnostic performance of gadoxetic acid-enhanced MRI is superior to that of dynamic MDCT (17). In a recent comparative study between C-arm CBCT and gadoxetic acid-enhanced MRI, the diagnostic performance of gadoxetic acid-enhanced MRI was significantly better than that of C-arm CBCT for HCC detection (mean Az = 0.890 vs. 0.681, respectively; $p < 0.001$) (18). However, in small HCCs (≤ 1 cm in diameter), C-arm CBCT showed a higher sensitivity (90.9% vs. 70.5%, $p = 0.023$) but a lower positive predictive value (40.8% vs. 57.4%, $p = 0.073$) than gadoxetic acid-enhanced MRI (Fig. 2) (18). These results indicate that C-arm CBCT can identify small HCCs as well as small non-tumorous enhancing lesions, such as an arterioportal shunt, aberrant venous drainage, or partial volume of an enhancing vessel (Fig. 3). C-arm CBCT allows a slice thickness and in-plane resolution of less than 0.3 mm as mentioned earlier. Therefore, it would be appropriate to assume that the better depiction of small hypervascular lesions on C-arm CBCT results from its high spatial resolution. Thus, the interventional radiologist needs to be careful regarding the diagnosis and in treatment planning of small (≤ 1 cm in diameter) hypervascular lesions detected on C-arm CBCT during chemoembolization.

C-arm CBCT can identify tumor-feeding arteries better than digital subtraction angiography (DSA) (Fig. 4). Meyer et al. (19) reported that the number of vessels identified as tumor feeders in each patient was significantly higher using additional C-arm CBCT than on angiography alone (4.0 ± 1.7 vs. 3.3 ± 1.4; $p = 0.003$). Iwazawa et al. (20) reported that the sensitivity, specificity, and accuracy of C-arm CBCT concerning identification of tumor-feeding arteries (96.9%, 97.0%, and 96.9%, respectively) were significantly higher than those for DSA (77.2%, 73.0%, and 75.4%, respectively).

The origin of the caudate artery is variable and is usually near the proximal hepatic arteries. Without the aid of C-arm CBCT, multiple selective angiography runs are needed to identify the caudate artery. Choi et al. (21) reported that C-arm CBCT obtained at the proper hepatic artery showed the caudate artery supplying HCCs in 92.3% of patients. Since the caudate artery originates from the proximal hepatic artery, C-arm CBCT obtained at lobar artery or segmental artery may miss the caudate artery.

Automated Vessel Tracking System

Recently, vessel identification software using CBCT data has been developed, and Wang et al. (22) reported on the high detectability of the cystic artery with a 3D vessel tracking system compared with 2D DSA images. Detectability rates of subsegmental tumor-feeders by vessel tracking software are reported to be 81–93% (23-26), higher than those by using DSA. C-arm CBCT and vessel tracking software may reduce the number of DSA runs required to identify tumor-feeding arteries. One disadvantage of the automated vessel tracking system is its false-positive results, resulting in unnecessary catheterization into these branches. Automated vessel tracking software provides an objective second opinion and the operator may be advised by this software, but the final decision concerning tumor-feeders should be made by operators themselves after a review of multiplanar images and 3D images.

When a tumor feeder is very thin, less than 1 mm, or if there is iodized oil accumulation adjacent to the viable tumor, the sensitivity of this software decreases significantly (26). For target definition, a circular regions of interest (ROI) is applied to cover the entire tumor. If a circular ROI is relatively bigger than the tumor or the shape of the target tumor is irregular, the target definition process

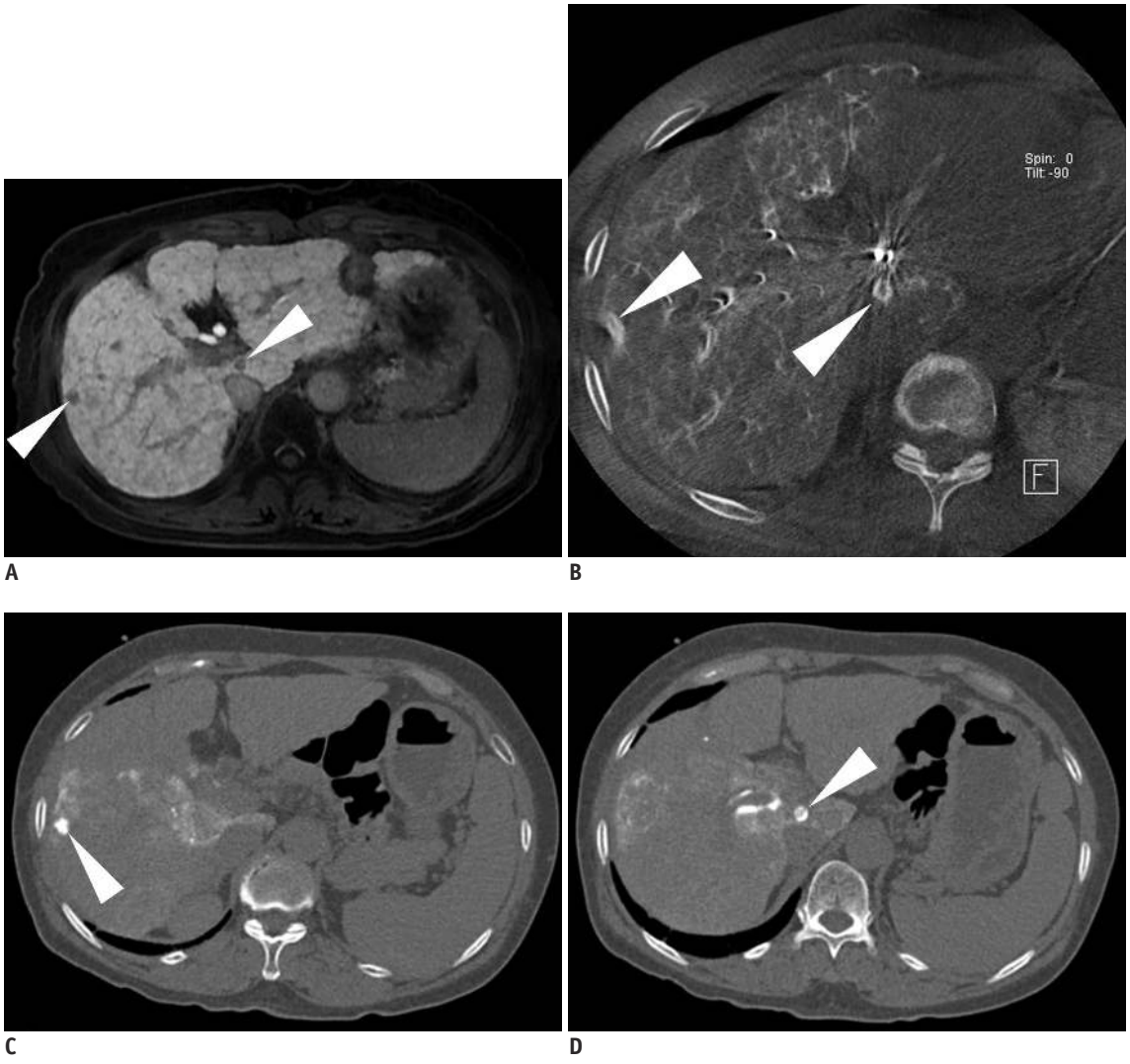

Fig. 2. 58-year-old woman with hepatocellular carcinoma.
A. Hepatobiliary phase image of gadoxetic acid-enhanced MRI shows two small nodules of hypointensity (arrowheads). These two nodules show no enhancement on arterial phase images of MRI and on arterial phase of CT scan (not shown). **B.** Axial image of C-arm cone-beam CT shows enhancement of these two nodules (arrowheads). Note motion artifact of hepatic artery caused by inadequate breath-hold. **C, D.** Unenhanced CT scan images obtained immediately after chemoembolization show dense accumulation of iodized oil in these two nodules (arrowheads) with surrounding parenchymal accumulation of iodized oil.

may be confused and false results may increase (26). These issues may be solved in the near future.

Prevention of Non-Target Embolization

Non-target embolization consists of three kinds of embolization; first, embolization of the hepatic artery which does not supply the HCCs, second, embolization of the non-hepatic artery originating from the hepatic artery, and third, embolization of extrahepatic collateral artery which does not feed HCCs.

Because hepatic arteries almost always overlap each other on 2D angiography, multiple selective angiograms of segmental or subsegmental hepatic arteries with oblique projections are needed to determine that the hepatic artery does not supply HCCs. 3D images of C-arm CBCT, including volume rendering images, can clearly show naïve hepatic arteries overlapping a tumor-feeding artery. There are several non-hepatic arteries originating from the hepatic artery, including the accessory left gastric artery, right gastric artery, cystic artery, falciform artery, and left inferior phrenic artery (27). Chemoembolization using iodized oil through these non-hepatic arteries infrequently cause clinically serious complications. Recently, serious complications requiring surgical management such as gall bladder infarct and radiation gastritis have been reported after more potent intra-arterial treatments such as drug-

Korean Journal of Radiology
KJR

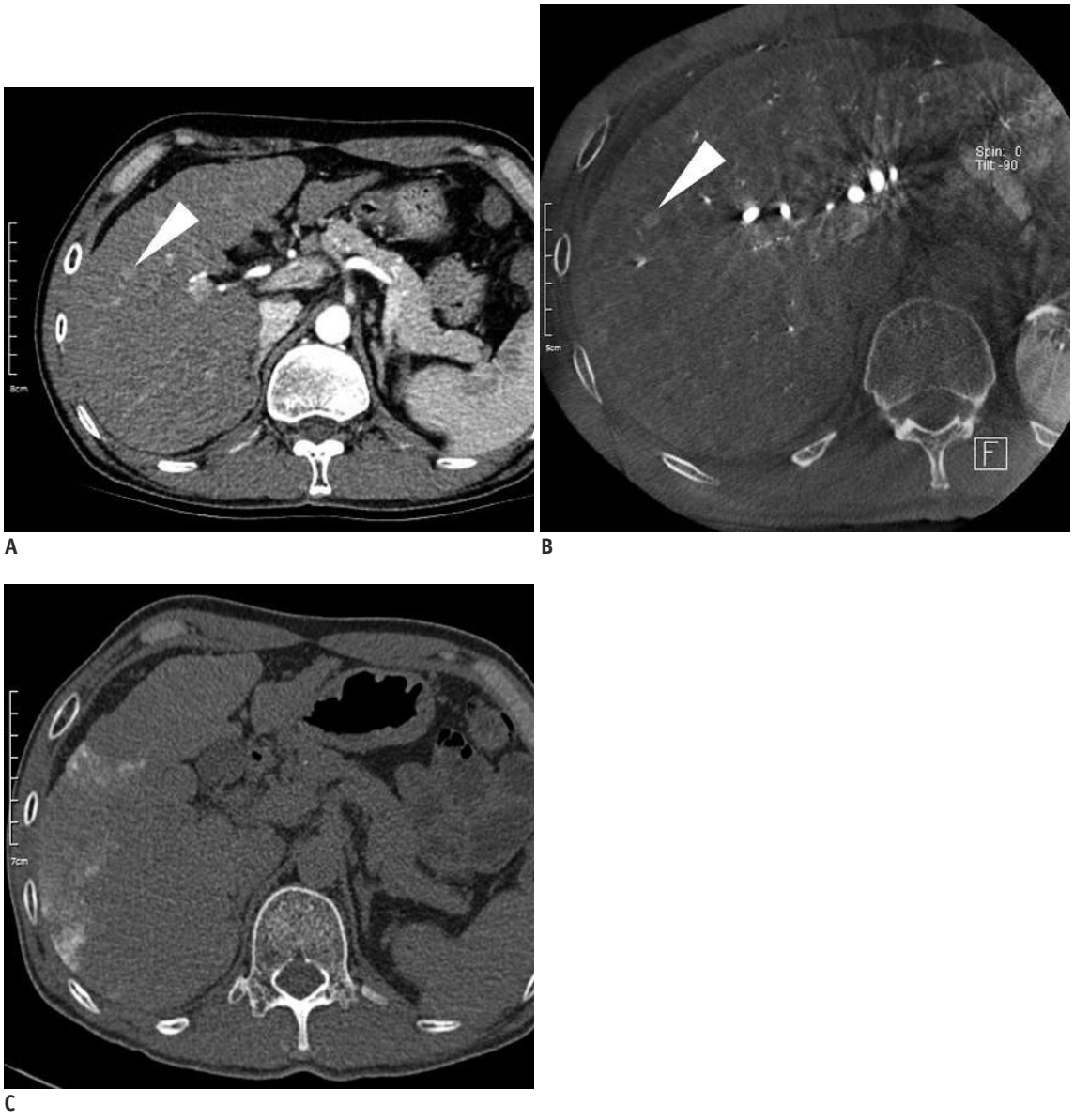

A B C

Fig. 3. 42-year-old man with hepatocellular carcinoma.
A. Axial CT scan shows small subtle enhancing lesion (arrowhead) in right lobe of liver. Wash-out of this nodule is equivocal on delayed image. **B.** Axial image of C-arm cone-beam CT shows subtle nodular enhancing lesion (arrowhead). This lesion was treated by iodized oil emulsion. **C.** Unenhanced CT scan obtained immediately after chemoembolization shows no nodular accumulation of iodized oil. During 2-year follow-up, this subtle nodule has persisted on follow-up CT scan without morphological change, which was thought to be benign arterioportal shunt.

eluting beads and radioactive beads had been used (5).

There are many extrahepatic collateral arteries that may supply HCCs. The most common one is the right inferior phrenic artery. The azygoesophageal branch of the right inferior phrenic artery almost always supplies systemic-to-pulmonary shunts that can mimic tumor staining (28). The superior adrenal artery, the first tributary of the right inferior phrenic artery, shows adrenal gland staining that may be confused for tumor staining.

C-arm CBCT can provide information concerning tumor staining and its feeding vessel, including a non-hepatic artery off the hepatic artery, a non-tumorous staining fed by hepatic or extrahepatic collateral artery, and vascular anatomy (28-30), resulting in prevention of non-target embolization.

Detection of Extrahepatic Collateral Artery Supplying HCCs

The suggestive findings of extrahepatic collateral artery supplying HCCs includes a large tumor in a peripheral location, hypertrophied extrahepatic collateral artery, and peripheral viable/recurred tumor of a previously

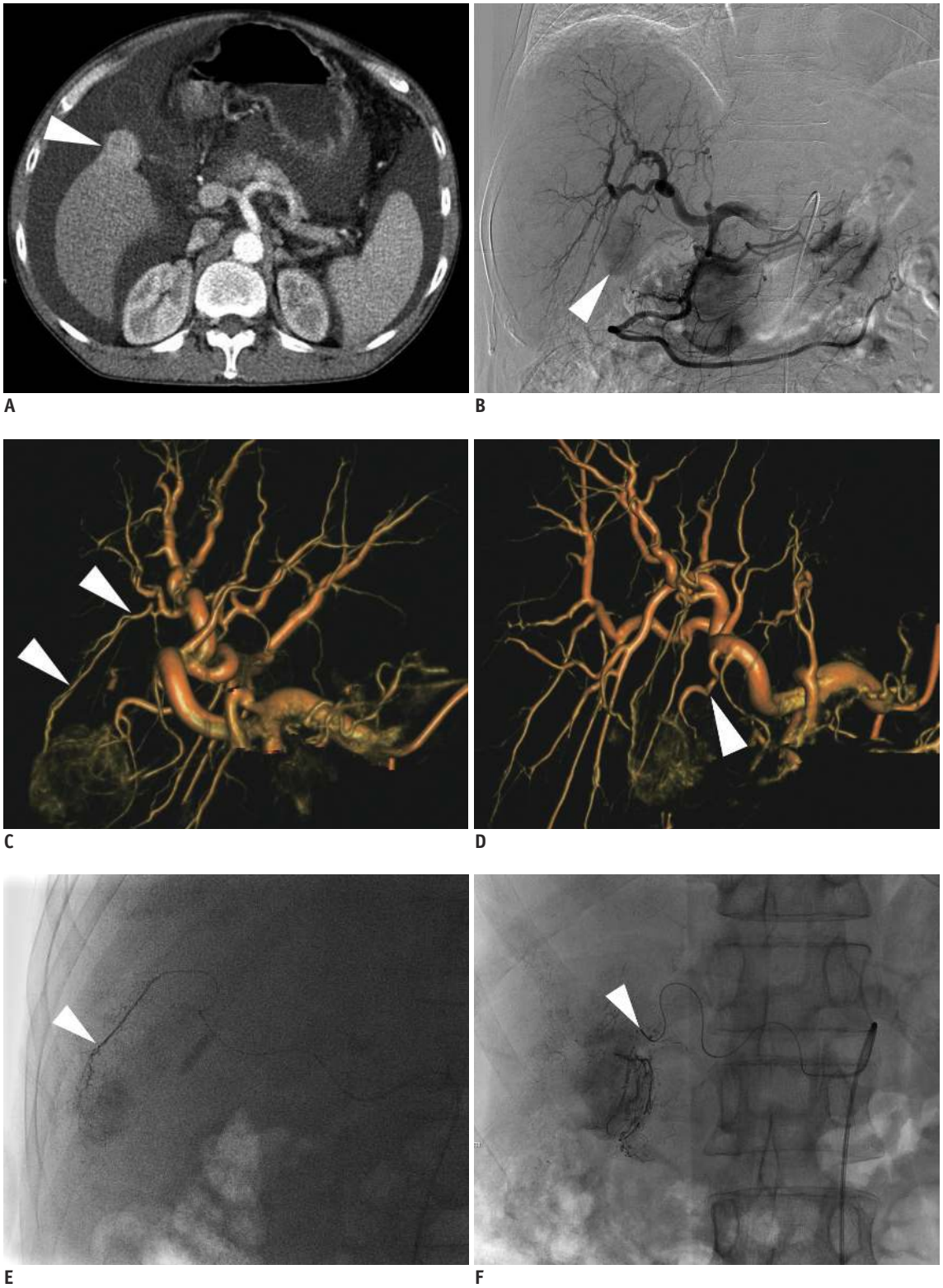

Fig. 4. 47-year-old man with hepatocellular carcinoma and Child-Pugh C class disease.
A. Axial CT scan shows exophytic enhancing nodule (arrowhead) in gallbladder bed. **B.** Celiac angiography shows tumor staining (arrowhead). **C.** Volume-rendering image of C-arm cone-beam CT with left anterior oblique projection of 30 degree shows tumor-feeding artery from S5 hepatic artery (arrowheads). **D.** Volume-rendering image of C-arm cone-beam CT with right anterior oblique projection of 20 degree and cranial oblique projection of 15 degree shows tumor-feeding artery from deep cystic artery (arrowhead). **E.** Spot image during chemoembolization shows tip (arrowhead) of microcatheter advanced into S5 hepatic artery. **F.** Spot image during chemoembolization shows tip (arrowhead) of microcatheter advanced into deep cystic artery.

Korean Journal of Radiology
KJR

treated lesion on CT/MR, and missing tumor staining on angiography (31). When there are multiple small tumors or a large tumor with minimal blood supply by an extrahepatic collateral artery, it is hard to perceive the presence of extrahepatic collateral artery on 2D angiography. Comparison between preprocedural CT/MR and an axial image of C-arm CBCT can clearly show a non-enhancing small tumor or unenhanced part within a larger tumor, which indicates the presence of an extrahepatic collateral artery supplying the tumors (Fig. 5).

Endpoint of Chemoembolization

One advantage of C-arm CBCT is the instant monitoring of the distribution of iodized oil. The goal of chemoembolization for HCC is that the entire target tumor is embolized with an adequate safety margin. CBCT during chemoembolization can confirm the distribution of iodized oil, so operators can decide whether or not the endpoints of chemoembolization have been reached. Iwazawa et al. (32) reported that C-arm CBCT is nearly equivalent to MDCT for detecting incomplete iodized oil accumulation after chemoembolization. Miyayama et al. (33) reported that local recurrence after chemoembolization for small HCCs could be reduced by intraprocedural monitoring of the embolized area.

The recent use of drug-eluting beads in chemoembolization may limit this ability of instant monitoring of iodized oil accumulation in the tumor because drug-eluting beads are radiolucent. However, even when drug-eluting beads are used, retention of contrast agents in the tumor can be observed on C-arm CBCT after embolization. A higher marginal contrast saturation observed on C-arm CBCT is correlated with a better short-term tumor response (34).

Clinical Outcome

In the literature, CBCT can provide information on changing the chemoembolization procedures in 19–50% of patients with HCC that was planned with DSA alone (7, 19, 35, 36). These modifications of procedure by C-arm CBCT can improve tumor response and patients' survival. Miyayama et al. (33) reported that the cumulative local recurrence rates in patients receiving chemoembolization by DSA alone were significantly higher than those in patients who underwent C-arm CBCT. Iwazawa et al. (37) also reported that the overall survival rates of patients who underwent chemoembolization with and without C-arm CT assistance were 94% and 79%, 81% and 65%, and 71% and 44% at 1, 2, and 3 years, respectively. Local progression-free survival rates of these patients were 43% and 27%, 31% and 10%, and 26% and 5% at 1, 2, and 3 years, respectively. Multivariate analysis showed that C-arm CT assistance was an independent factor associated with longer overall survival (hazard ratio, 0.40; $p = 0.033$) and local progression-free survival (hazard ratio, 0.25; $p = 0.003$).

Radiation Dose of C-Arm CBCT

Routine use of C-arm CBCT can increase stochastic risk (i.e., radiation-induced cancer) because of the additional radiation exposure. However, Kothary et al. (38) demonstrated that C-arm CBCT can replace some angiographic runs, thereby resulting in a negligible increase in dose-area product which is considered an adequate surrogate for stochastic risks. In addition, C-arm CBCT decreases skin dose exposure because it is concentrated to the right upper abdomen, distributing the skin dose of radiation over a range of 210°, resulting in decreased deterministic risk (i.e., radiation-induced skin injury).

Limitations of C-Arm CBCT

C-arm CBCT has small field of view, so the liver was entirely covered by C-arm CBCT in only 29% of cases (39). The field of view in CBCT scanning should be individually adjusted to include target tumors and the region of interest. In patients with large livers containing bilobar disease, two or more acquisitions of the CBCT is mandatory.

Cone-beam computed tomography images have motion artifacts caused by inadequate breath-holding and cardiac motion. In one report, 3% of patients could not cooperate with breathing instructions and were unable to undergo CBCT scanning (39). CBCT images are severely deteriorated by respiratory motion artifacts or cardiac motion in 5–10% of patients (7, 39). Cardiac motion can deteriorate CBCT image quality in the left lateral segments, especially in S2. Even in patients with good breath-holding, 25% of S2 hepatic arteries suffer from motion artifact caused by cardiac motion (39).

CONCLUSION

C-arm CBCT can provide additional useful information about HCCs and their feeding arteries and can be used as

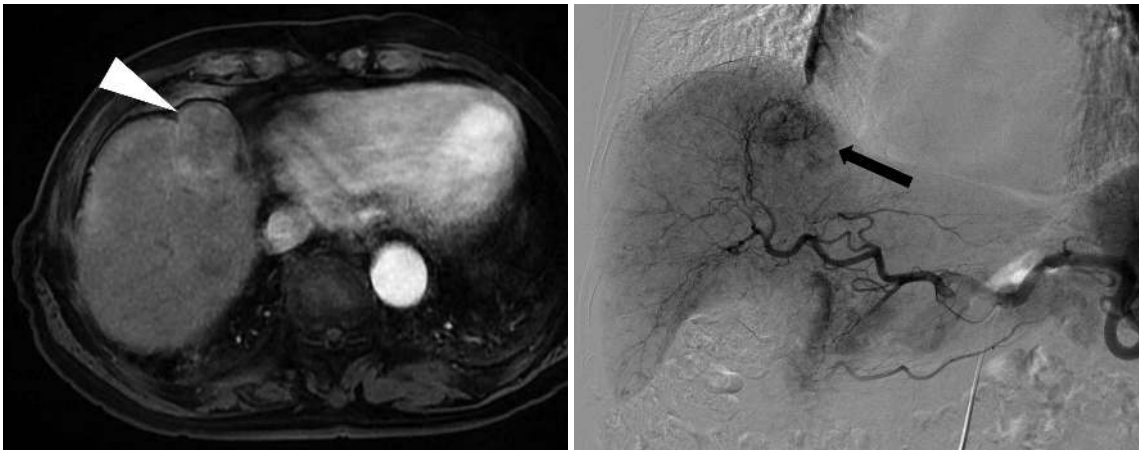

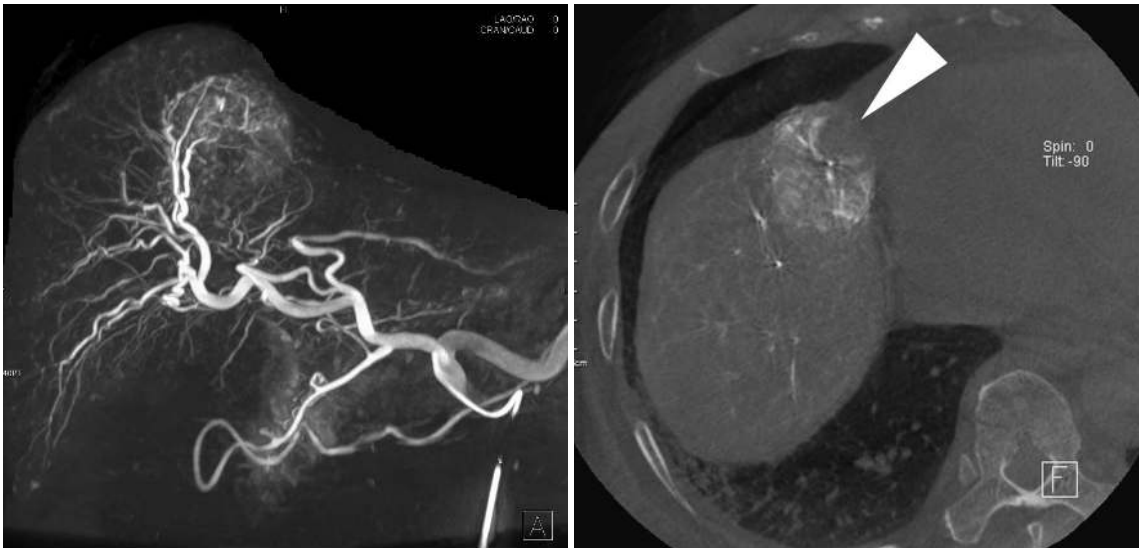

Fig. 5. 78-year-old man with hepatocellular carcinoma.
A. Arterial phase images of gadoxetic acid-enhanced MRI shows exophytic nodule (arrowhead) with faint enhancement. **B.** Celiac angiography shows hypervascular tumor staining (arrow). **C.** Maximum-intensity-projection image of C-arm cone-beam CT shows hypervascular tumor staining. **D.** Axial image of C-arm cone-beam CT shows non-enhancing part (arrowhead) of tumor which suggests presence of extrahepatic collateral artery supplying tumor. **E.** Angiography of right inferior phrenic artery shows tumor staining (arrowhead).

Korean Journal of Radiology
KJR

navigational tools with 3D roadmapping. The combination of current and future capabilities of C-arm CBCT may improve the efficacy and safety of chemoembolization and may widen the indication of chemoembolization. C-arm CBCT may improve the prognosis of HCC patients when interventional radiologists adopt this next generation of imaging technology to their daily clinical practice.

REFERENCES

1. Shin SW. The current practice of transarterial chemoembolization for the treatment of hepatocellular carcinoma. *Korean J Radiol* 2009;10:425-434
2. Cheung JY, Kim Y, Shim SS, Lim SM. Combined fluoroscopy- and CT-guided transthoracic needle biopsy using a C-arm cone-beam CT system: comparison with fluoroscopy-guided biopsy. *Korean J Radiol* 2011;12:89-96
3. Georgiades CS, Hong K, Geschwind JF, Liddell R, Syed L, Kharlip J, et al. Adjunctive use of C-arm CT may eliminate technical failure in adrenal vein sampling. *J Vasc Interv Radiol* 2007;18:1102-1105
4. Kakeda S, Korogi Y, Ohnari N, Moriya J, Oda N, Nishino K, et al. Usefulness of cone-beam volume CT with flat panel detectors in conjunction with catheter angiography for transcatheter arterial embolization. *J Vasc Interv Radiol* 2007;18:1508-1516
5. Collins J, Salem R. Hepatic radioembolization complicated by gastrointestinal ulceration. *Semin Intervent Radiol* 2011;28:240-245
6. Orth RC, Wallace MJ, Kuo MD; Technology Assessment Committee of the Society of Interventional Radiology. C-arm cone-beam CT: general principles and technical considerations for use in interventional radiology. *J Vasc Interv Radiol* 2008;19:814-820
7. Tognolini A, Louie JD, Hwang GL, Hofmann LV, Sze DY, Kothary N. Utility of C-arm CT in patients with hepatocellular carcinoma undergoing transhepatic arterial chemoembolization. *J Vasc Interv Radiol* 2010;21:339-347
8. Wallace MJ, Kuo MD, Glaiberman C, Binkert CA, Orth RC, Soulez G, et al. Three-dimensional C-arm cone-beam CT: applications in the interventional suite. *J Vasc Interv Radiol* 2008;19:799-813
9. Koelblinger C, Schima W, Berger-Kulemann V, Wolf F, Plank C, Weber M, et al. C-arm CT during hepatic arteriography tumour-to-liver contrast: intraindividual comparison of three different contrast media application protocols. *Eur Radiol* 2013;23:938-942
10. Miyayama S, Yamashiro M, Okuda M, Yoshie Y, Nakashima Y, Ikeno H, et al. Detection of corona enhancement of hypervascular hepatocellular carcinoma by C-arm dual-phase cone-beam CT during hepatic arteriography. *Cardiovasc Intervent Radiol* 2011;34:81-86
11. Loffroy R, Lin M, Yenokyan G, Rao PP, Bhagat N, Noordhoek N, et al. Intraprocedural C-arm dual-phase cone-beam CT: can it be used to predict short-term response to TACE with drug-eluting beads in patients with hepatocellular carcinoma? *Radiology* 2013;266:636-648
12. Higashihara H, Osuga K, Onishi H, Nakamoto A, Tsuboyama T, Maeda N, et al. Diagnostic accuracy of C-arm CT during selective transcatheter angiography for hepatocellular carcinoma: comparison with intravenous contrast-enhanced, biphasic, dynamic MDCT. *Eur Radiol* 2012;22:872-879
13. Meyer BC, Frericks BB, Voges M, Borchert M, Martus P, Justiz J, et al. Visualization of hypervascular liver lesions During TACE: comparison of angiographic C-arm CT and MDCT. *AJR Am J Roentgenol* 2008;190:W263-W269
14. Iwazawa J, Ohue S, Hashimoto N, Abe H, Hamuro M, Mitani T. Detection of hepatocellular carcinoma: comparison of angiographic C-arm CT and MDCT. *AJR Am J Roentgenol* 2010;195:882-887
15. Miyayama S, Yamashiro M, Okuda M, Yoshie Y, Sugimori N, Igarashi S, et al. Usefulness of cone-beam computed tomography during ultraselective transcatheter arterial chemoembolization for small hepatocellular carcinomas that cannot be demonstrated on angiography. *Cardiovasc Intervent Radiol* 2009;32:255-264
16. Loffroy R, Lin M, Rao P, Bhagat N, Noordhoek N, Radaelli A, et al. Comparing the detectability of hepatocellular carcinoma by C-arm dual-phase cone-beam computed tomography during hepatic arteriography with conventional contrast-enhanced magnetic resonance imaging. *Cardiovasc Intervent Radiol* 2012;35:97-104
17. Onishi H, Kim T, Imai Y, Hori M, Nagano H, Nakaya Y, et al. Hypervascular hepatocellular carcinomas: detection with gadoxetate disodium-enhanced MR imaging and multiphasic multidetector CT. *Eur Radiol* 2012;22:845-854
18. Yu MH, Kim JH, Yoon JH, Kim HC, Chung JW, Han JK, et al. Role of C-arm CT for transcatheter arterial chemoembolization of hepatocellular carcinoma: diagnostic performance and predictive value for therapeutic response compared with gadoxetic acid-enhanced MRI. *AJR Am J Roentgenol* 2013;201:675-683
19. Meyer BC, Witschel M, Frericks BB, Voges M, Hopfenmüller W, Wolf KJ, et al. The value of combined soft-tissue and vessel visualisation before transarterial chemoembolisation of the liver using C-arm computed tomography. *Eur Radiol* 2009;19:2302-2309
20. Iwazawa J, Ohue S, Mitani T, Abe H, Hashimoto N, Hamuro M, et al. Identifying feeding arteries during TACE of hepatic tumors: comparison of C-arm CT and digital subtraction angiography. *AJR Am J Roentgenol* 2009;192:1057-1063
21. Choi WS, Kim HC, Hur S, Choi JW, Lee JH, Yu SJ, et al. Role of C-arm CT in identifying caudate arteries supplying hepatocellular carcinoma. *J Vasc Interv Radiol* 2014;25:1380-1388
22. Wang X, Shah RP, Maybody M, Brown KT, Getrajdman GI, Stevenson C, et al. Cystic artery localization with a three-dimensional angiography vessel tracking system compared

with conventional two-dimensional angiography. *J Vasc Interv Radiol* 2011;22:1414-1419
23. Deschamps F, Solomon SB, Thornton RH, Rao P, Hakime A, Kuoch V, et al. Computed analysis of three-dimensional cone-beam computed tomography angiography for determination of tumor-feeding vessels during chemoembolization of liver tumor: a pilot study. *Cardiovasc Intervent Radiol* 2010;33:1235-1242
24. Miyayama S, Yamashiro M, Ikuno M, Okumura K, Yoshida M. Ultraselective transcatheter arterial chemoembolization for small hepatocellular carcinoma guided by automated tumor-feeders detection software: technical success and short-term tumor response. *Abdom Imaging* 2014;39:645-656
25. Miyayama S, Yamashiro M, Hashimoto M, Hashimoto N, Ikuno M, Okumura K, et al. Identification of small hepatocellular carcinoma and tumor-feeding branches with cone-beam CT guidance technology during transcatheter arterial chemoembolization. *J Vasc Interv Radiol* 2013;24:501-508
26. Iwazawa J, Ohue S, Hashimoto N, Muramoto O, Mitani T. Clinical utility and limitations of tumor-feeder detection software for liver cancer embolization. *Eur J Radiol* 2013;82:1665-1671
27. Song SY, Chung JW, Lim HG, Park JH. Nonhepatic arteries originating from the hepatic arteries: angiographic analysis in 250 patients. *J Vasc Interv Radiol* 2006;17:461-469
28. Kim HC, Chung JW, Park JH, An S, Son KR, Seong NJ, et al. Transcatheter arterial chemoembolization for hepatocellular carcinoma: prospective assessment of the right inferior phrenic artery with C-arm CT. *J Vasc Interv Radiol* 2009;20:888-895
29. Kim HC, Chung JW, An S, Seong NJ, Jae HJ, Cho BH, et al. Left inferior phrenic artery feeding hepatocellular carcinoma: angiographic anatomy using C-arm CT. *AJR Am J Roentgenol* 2009;193:W288-W294
30. Kim HC, Chung JW, Lee IJ, An S, Seong NJ, Son KR, et al. Intercostal artery supplying hepatocellular carcinoma: demonstration of a tumor feeder by C-arm CT and multidetector row CT. *Cardiovasc Intervent Radiol* 2011;34:87-91
31. Kim HC, Chung JW, Lee W, Jae HJ, Park JH. Recognizing extrahepatic collateral vessels that supply hepatocellular carcinoma to avoid complications of transcatheter arterial chemoembolization. *Radiographics* 2005;25 Suppl 1:S25-S39
32. Iwazawa J, Ohue S, Kitayama T, Sassa S, Mitani T. C-arm CT for assessing initial failure of iodized oil accumulation in chemoembolization of hepatocellular carcinoma. *AJR Am J Roentgenol* 2011;197:W337-W342
33. Miyayama S, Yamashiro M, Hashimoto M, Hashimoto N, Ikuno M, Okumura K, et al. Comparison of local control in transcatheter arterial chemoembolization of hepatocellular carcinoma ≤6 cm with or without intraprocedural monitoring of the embolized area using cone-beam computed tomography. *Cardiovasc Intervent Radiol* 2014;37:388-395
34. Suk Oh J, Jong Chun H, Gil Choi B, Giu Lee H. Transarterial chemoembolization with drug-eluting beads in hepatocellular carcinoma: usefulness of contrast saturation features on cone-beam computed tomography imaging for predicting short-term tumor response. *J Vasc Interv Radiol* 2013;24:483-489
35. Virmani S, Ryu RK, Sato KT, Lewandowski RJ, Kulik L, Mulcahy MF, et al. Effect of C-arm angiographic CT on transcatheter arterial chemoembolization of liver tumors. *J Vasc Interv Radiol* 2007;18:1305-1309
36. Wallace MJ, Murthy R, Kamat PP, Moore T, Rao SH, Ensor J, et al. Impact of C-arm CT on hepatic arterial interventions for hepatic malignancies. *J Vasc Interv Radiol* 2007;18:1500-1507
37. Iwazawa J, Ohue S, Hashimoto N, Muramoto O, Mitani T. Survival after C-arm CT-assisted chemoembolization of unresectable hepatocellular carcinoma. *Eur J Radiol* 2012;81:3985-3992
38. Kothary N, Abdelmaksoud MH, Tognolini A, Fahrig R, Rosenberg J, Hovsepian DM, et al. Imaging guidance with C-arm CT: prospective evaluation of its impact on patient radiation exposure during transhepatic arterial chemoembolization. *J Vasc Interv Radiol* 2011;22:1535-1543
39. Lee IJ, Chung JW, Yin YH, Kim HC, Kim YI, Jae HJ, et al. Cone-beam CT hepatic arteriography in chemoembolization for hepatocellular carcinoma: angiographic image quality and its determining factors. *J Vasc Interv Radiol* 2014;25:1369-1379; quiz 1379-1379.e1